



Original article

Exploiting the lipoic acid structure in the search for novel multitarget ligands against Alzheimer's disease

Michela Rosini^{a,*}, Elena Simoni^a, Manuela Bartolini^a, Andrea Tarozzi^b, Riccardo Matera^a, Andrea Milelli^a, Patrizia Hrelia^b, Vincenza Andrisano^a, Maria Laura Bolognesi^a, Carlo Melchiorre^a

^a Department of Pharmaceutical Sciences, University of Bologna, Via Belmeloro 6, 40126 Bologna, Italy

^b Department of Pharmacology, University of Bologna, Via Irnerio 48, 40126 Bologna, Italy

ARTICLE INFO

Article history:

Received 12 April 2011

Received in revised form

31 August 2011

Accepted 1 September 2011

Available online 7 September 2011

Keywords:

Lipoic acid

Lipocrine's enantiomers

Alzheimer's disease

Antioxidants

Acetylcholinesterase

Multitarget compounds

ABSTRACT

Lipoic acid (LA) is a natural antioxidant. Its structure was previously combined with that of the acetylcholinesterase inhibitor tacrine to give lipocrine (**1**), a lead compound multitargeted against Alzheimer's disease (AD). Herein, we further explore LA as a privileged structure for developing multimodal compounds to investigate AD. First, we studied the effect of LA chirality by evaluating the cholinesterase profile of **1**'s enantiomers. Then, a new series of LA hybrids was designed and synthesized by combining racemic LA with motifs of other known anticholinesterase agents (rivastigmine and memoquin). This afforded **4**, which represents a step forward in the search for balanced anticholinesterase and antioxidant capacities.

© 2011 Elsevier Masson SAS. All rights reserved.

1. Introduction

Alzheimer's disease (AD^a) is the most common form of irreversible dementia, for which effective treatments are urgently needed. AD is thought to be a complex, multifactorial syndrome with many related molecular lesions contributing to its pathogenesis [1]. Besides the pathological hallmarks of the disease, which include the accumulation of misfolded protein deposits as amyloid- β (A β) plaques and neurofibrillary tangles, AD brains exhibit constant evidence of oxidative damage [2]. In particular, oxidative injury is observed in the CNS of AD patients in almost every class of cellular macromolecules, including nucleic acids, proteins, and lipids. This has been used to support the "oxidative stress hypothesis" of AD. Positing reactive oxygen species (ROS) as playing a key role in AD onset and progression, this hypothesis proposes antioxidants as beneficial therapeutic tools in AD treatment [3,4].

To date, a variety of antioxidants have been examined as neuroprotectants. Animal models and most human epidemiological studies have supported the assumption of a correlation between antioxidant intake and cognitive function. However, randomized clinical trials have generally afforded disappointing results [2,5].

In light of these conflicting data, there are growing calls for a critical rethinking of the oxidative stress hypothesis. Experimental evidence has recently expanded our knowledge of the role of oxidative stress, corroborating the functional importance of oxidative imbalance as a crucial and early event in mediating the AD pathogenesis [6], and indicating the complexity of the redox system *in vivo* as a nodal point [2].

ROS production is due to a variety of different sources including mitochondrial abnormalities, unbound transition metals, and A β peptides themselves [7]. Interestingly, all of these factors are strictly correlated and establish interconnections with other key events of AD, such as apoptosis, A β processing and secretion, τ phosphorylation, and the disruption of calcium homeostasis [8]. This complex scenario may explain why simple antioxidants did not provide effective therapies for AD treatment, prompting researchers to follow new trends in antioxidant development.

In particular, antioxidants presenting additional pharmacological effects are currently thought to offer a good chance of combating complex diseases in which free radicals are significant

Abbreviations: AD, Alzheimer's disease; A β , amyloid- β ; ROS, reactive oxygen species; MTDLs, multitarget-directed ligands; LA, lipoic acid; AChE, acetylcholinesterase; BuChE, butyrylcholinesterase; PAS, peripheral anionic site.

* Corresponding author. Tel.: +39 0512099722; fax: +39 0512099734.

E-mail address: michela.rosini@unibo.it (M. Rosini).

Table 1
Inhibition of cholinesterases activity by (R)-1, (S)-1, 2–6 and reference compounds.

Compounds	IC ₅₀ (M) ^a ±SEM hAChE	IC ₅₀ (M) ^a ±SEM hBuChE
1^b	(2.53 ± 0.16) × 10 ⁻¹⁰	(1.08 ± 0.25) × 10 ⁻⁸
(S)-1	(4.71 ± 0.17) × 10 ⁻¹⁰	(1.21 ± 0.03) × 10 ⁻⁸
(R)-1	(2.30 ± 0.15) × 10 ⁻¹⁰	(1.26 ± 0.14) × 10 ⁻⁸
2	(2.66 ± 0.23) × 10 ⁻⁹	(3.06 ± 0.07) × 10 ⁻⁸
3	(1.92 ± 0.25) × 10 ⁻⁴	(2.05 ± 0.02) × 10 ⁻⁴
4	(2.56 ± 0.08) × 10 ⁻⁷	(2.49 ± 0.11) × 10 ⁻⁶
5	(7.41 ± 0.37) × 10 ⁻⁵	(3.98 ± 0.24) × 10 ⁻⁷
6	(2.52 ± 0.17) × 10 ⁻⁵	(8.24 ± 0.65) × 10 ⁻⁵
memoquin ^c	(1.55 ± 0.11) × 10 ⁻⁹	(1.44 ± 0.10) × 10 ⁻⁶
rivastigmine ^d	(3.03 ± 0.21) × 10 ⁻⁶	(3.01 ± 0.14) × 10 ⁻⁷
LA ^b	> 10 ⁻³	> 10 ⁻³

^a Human recombinant AChE and BuChE from human serum were used. IC₅₀ values represent the concentration of inhibitor required to decrease enzyme activity by 50% and are the mean of two independent measurements, each performed in triplicate.

^b From ref. [18].

^c From ref. [21].

^d From ref. [22]; SEM = Standard Error of the Mean.

but not exclusive drivers [9]. This concept has been recently rationalized in the field of neurodegenerative diseases affording the multitarget-directed ligands (MTDLs) design strategy. This strategy holds that single molecules, endowed with antioxidant properties and able to act at different steps in the neurodegenerative process, can produce additive neuroprotective effects against AD [10,11].

Lipoic acid (LA) is a natural occurring antioxidant. Its antioxidant activity is attributed to its ability to scavenge free radicals in both membrane and aqueous domains. It does this by chelating redox-active transition metals, increasing the levels of reduced glutathione and down-regulating inflammatory processes [12,13]. LA has also been shown to possess a variety of additional properties which can interfere with the pathogenic principles of AD [14]. Moreover, LA is readily absorbed by diet, transported, taken up by cells, and reduced to the active dihydrolipoic acid in various tissues, including brain [15]. Therefore, LA could be considered a privileged structure in designing new MTDLs for the investigation and, conceivably, treatment of AD [15–17].

In 2005, with this in mind, we developed lipocrine (**1**), one of the first multifunctional antioxidants rationally designed to combat AD [18]. **1** combined, in the same molecule, the structure of LA with a derivative of tacrine, the first AChE inhibitor approved for AD treatment. It was also argued that the cyclic moiety of LA could interact with the peripheral anionic site (PAS) of AChE, which is associated with the neurotoxic cascade underlying AD through AChE-induced Aβ aggregation. Indeed, kinetic analyses confirmed that **1** could bind both catalytic and peripheral sites, thus acting as a mixed type inhibitor [18].

Table 2
Effects of compounds on intracellular ROS formation in SH-SY5Y cells^a.

Conc. (μM)	Compounds					
	1	2	3	4	5	6
0	82.4 ± 6.6	82.4 ± 6.6	82.4 ± 6.6	82.4 ± 6.6	82.4 ± 6.6	82.4 ± 6.6
1	83.2 ± 7.4	81.0 ± 7.9	82.0 ± 7.6	80.8 ± 5.9	82.5 ± 6.5	80.3 ± 6.2
5	65.0 ± 6.2 ^b	79.8 ± 3.2	73.5 ± 6.5	75.8 ± 5.8	80.0 ± 5.2	76.8 ± 6.3
10	50.0 ± 5.5 ^c	80.2 ± 4.1	63.4 ± 5.6 ^b	69.6 ± 4.2 ^b	68.8 ± 5.5 ^b	48.0 ± 6.1 ^c
50	31.0 ± 4.9 ^d	Tox ^e	Tox ^e	37.6 ± 4.5 ^d	46.4 ± 5.0 ^c	34.4 ± 5.4 ^d

^a The results are expressed as a percentage increase of intracellular ROS induced by exposure to *t*-BuOOH. Values are reported as mean ± SD of three/four independent experiments.

^b *p* < 0.05.

^c *p* < 0.01.

^d *p* < 0.001 vs untreated at ANOVA with Dunnett post hoc test.

^e Tox = cytotoxic.

In *in vitro* models, **1** effectively displayed the expected multiple biological properties, namely inhibition of AChE activity, inhibition of AChE-induced Aβ aggregation, and ability to protect cells against ROS (Tables 1 and 2), emerging as a candidate for drug development [19].

In light of this, we wanted to expand the study that afforded **1** and its derivatives by exploiting the LA structure in the search for novel MTDLs against AD. To this end, we first studied the contribution of LA and tetrahydroacridine portions to the observed multimodal profile of **1**. It has been reported that stereochemistry is not relevant for the protective effect of LA against oxidative cell damage [20]. However, to verify whether it affects cholinesterase inhibition, the two enantiomers of **1**, (S)-1 and (R)-1 were synthesized and studied. Moreover, to confirm the hypothesis that the dithiolane function is indeed responsible for the antioxidant profile of LA adducts, a thiophene analogue of **1** was synthesized, affording **2** (Fig. 1).

Then, we investigated the role of the 9-amino-6-chloro-1,2,3,4-tetrahydroacridine fragment, by replacing it with a 2-chloro-4-amino-6,7-dimethoxy-quinazoline moiety to give **3** (Fig. 1). The quinazoline function was selected to verify if a chloro-substituted aromatic group, protonated at physiological pH, was a sufficient requisite for AChE binding. Then, we focused on designing new LA adducts in which the antioxidant moiety was conjugated with the structural features of other classical AChE inhibitors. Thus, in the present study, we linked LA with the anticholinesterase motifs of the marketed drug rivastigmine and memoquin, an AD drug candidate developed in our group [21,22]. This afforded the hybrid compounds **4–6** (Fig. 1). The selection of the pharmacophoric features from the abovementioned anticholinesterase inhibitors deserves comment. We focused on the benzylamino function, a feature common to both prototypes. This feature has already proven effective in recognizing the AChE catalytic site for memoquin and its derivatives [21,23] and for a class of polyamine-based noncovalent inhibitors [24–28]. Thus, combining a *N*¹-ethyl-*N*¹-(2-methoxy-benzyl)-hexane-1,6-diamine moiety with LA provided **4**. Similarly, although the peculiar mode of inhibition of rivastigmine is related to its carbamic function, we envisioned that the 3-(1-(dimethylamino)ethyl)phenol group could also provide a recognition fragment for the AChE active site. As further support, docking studies previously showed that this moiety is itself a competitive AChE inhibitor [29]. Consequently, the 3-(1-(dimethylamino)ethyl)phenol group should endow **5** and **6** with a binding mode similar to that of **1** and the other derivatives, i.e. a reversible mixed type inhibition of AChE, with LA possibly interacting with the PAS of the enzyme.

Synthesized compounds were then investigated to assess their antioxidant, anticholinesterase, and anti-aggregating activities.

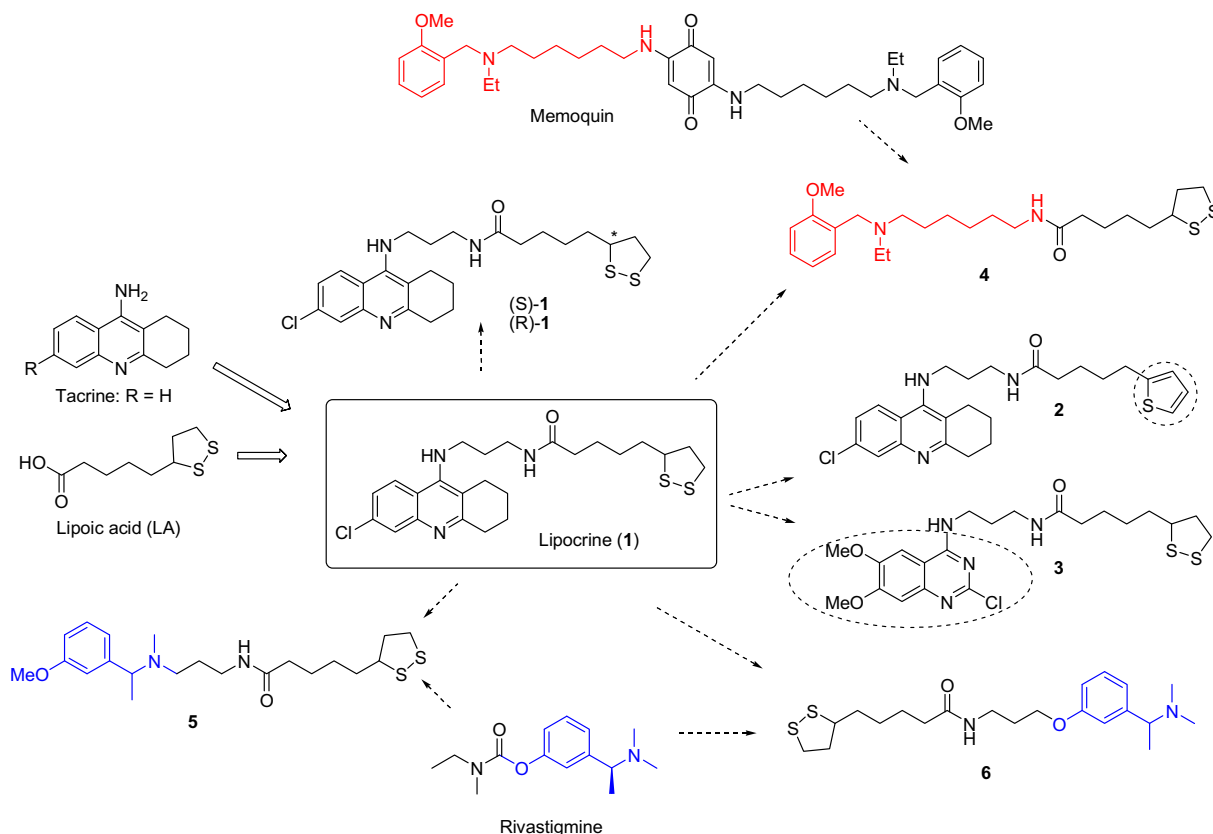


Fig. 1. Design strategy for compounds (R)-1, (S)-1, and 2–6.

2. Chemistry

We have previously reported how a coupling reaction of amines with LA provides easy access to a variety of derivatives [18,30,31]. Following the same procedure, we here synthesized 2–6 by coupling intermediates 7 [18], 9, 10 [22], 13 and 16 with LA or 5-(thiophen-2-yl)pentanoic acid in the presence of 1-(3-dimethylaminopropyl)-3-ethylcarbodiimide hydrochloride (EDCI) (Scheme 1). 13 and 16 were obtained through alkylation with *tert*-butyl 3-chloropropylcarbamate of 11 and 14, followed by removal of the BOC group with trifluoroacetic acid.

Concerning 5 and 6, diastereoisomers were not separated because of their weak AChE inhibitory potency.

(S)-1 and (R)-1 were synthesized according to the procedure previously reported for 1 [18], starting from 7 and (S)-lipoic acid or (R)-lipoic acid.

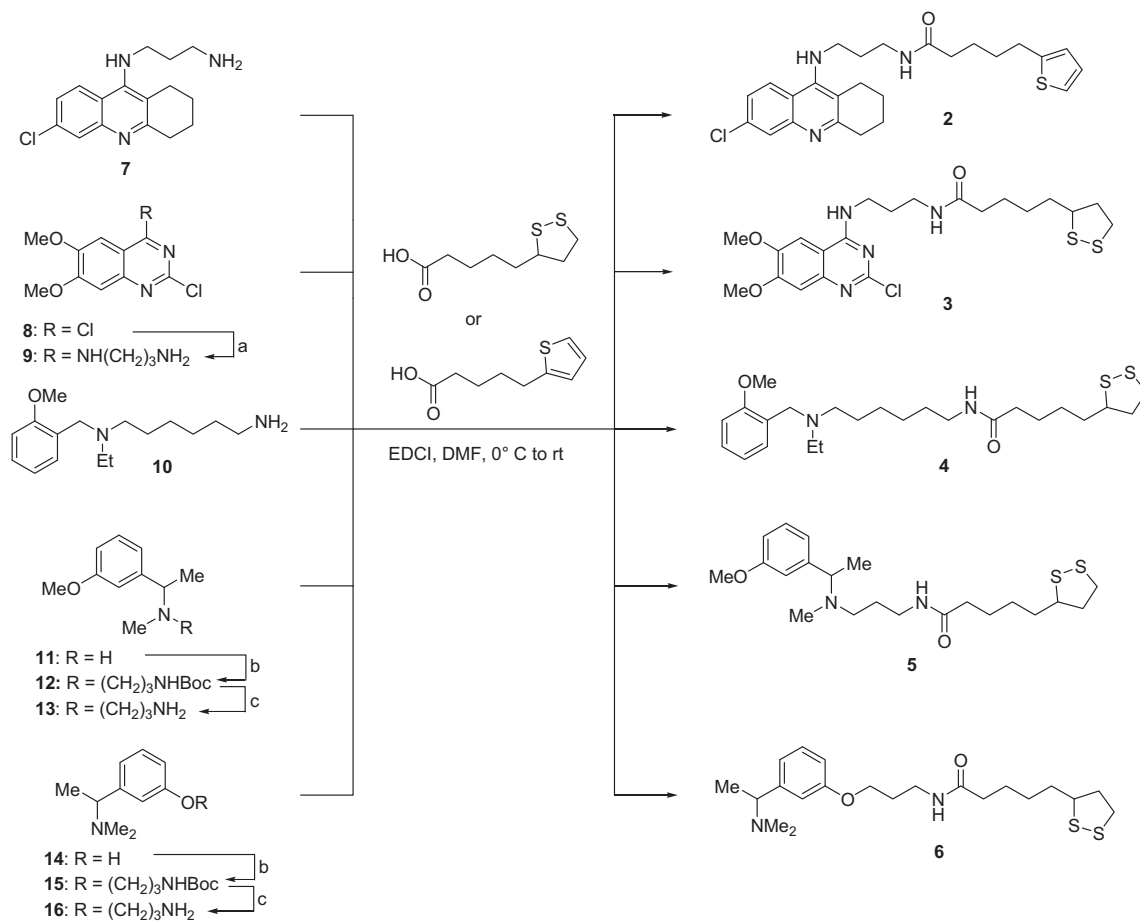
3. Results and discussion

As previously mentioned, the first step of the present study was to define the role of LA stereochemistry in the cholinesterase inhibition of 1. Thus, the two enantiomers of 1 ((S)-1 and (R)-1) were tested on human AChE and BuChE by the method of Ellman et al. [32]. Due to the lack of activity of racemic LA [18], its enantiomers were not tested. The obtained results clearly show that, while BuChE did not discriminate between (S)-1 and (R)-1, the inhibitory potencies of the two enantiomers were slightly different on AChE. (R)-1 was only twice as potent as (S)-1. Since there is no biologically relevant difference between racemic 1 and the most active enantiomer (R)-1, we decided to synthesize and study the LA adducts 2–6 as racemic compounds. We assessed the cholinesterase

inhibition profile of 2–6 with respect to prototypes 1, memoquin, rivastigmine, and LA (Table 1). The obtained data clearly highlight the role of the different moieties of 1 in AChE inhibition. Indeed, the Cl-tetrahydroacridine fragment of 1 emerged as a key feature for AChE binding, as revealed by the dramatic loss of efficacy observed for the quinazoline analogue 3. Conversely, the replacement of the dithiolane with a thiophene unit, affording 2, slightly affected AChE inhibition.

Of compounds 4–6, where the tacrine-like moiety of 1 was substituted with diverse anticholinesterase motifs, only 4 emerged as an effective AChE inhibitor, although it was considerably less potent than the prototype ($IC_{50} = 256 \pm 8$ nM and 0.253 ± 0.016 nM for 4 and 1, respectively). No significant anticholinesterase activity was confirmed for 5 and 6, which bear the 3-(1-(dimethylamino)ethyl)phenol function of rivastigmine. 4–6 share a benzylamino group and therefore a cationic head, which is a fundamental feature for cholinesterase recognition. However, only the *o*-methoxybenzylamino group of 4 was confirmed to effectively anchor the AChE catalytic site. Conversely, the 3-(1-(dimethylamino)ethyl)phenol moiety of 5 and 6, lacking the carbamate functionality of rivastigmine, seemed unable to properly interact with the AChE binding site.

Concerning the inhibition of BuChE, we note that, in general, structural modification led to a drop in the inhibitory activity of all LA-carrying derivatives except 5, which retained the sub-micromolar potency of the reference compound rivastigmine. Moreover, although 4 was less active than 1 on hBuChE, it still showed an inhibitory potency in the micromolar range, with a selectivity profile similar to that of 1 (BuChE/AChE = 10 and 43 for 4 and 1, respectively). Compound 5 was the only butyryl-selective derivative in the series. It could be useful in treating the



Scheme 1. Reaction conditions: (a) propanediamine, anhydrous THF, rt 12 h; (b) Cl(CH₂)₃NHBoc, K₂CO₃, KI, DMF, reflux 24 h; (c) TFA, CH₂Cl₂, rt 2 h.

moderate/severe form of AD where the BuChE/AChE ratio is deeply altered by disease progression and levels of AChE are too low for AChE inhibitors to be effective [33].

Our main goal was to identify a new antioxidant MTDL. To determine the potential interest of **2–6** for the treatment of AD, we thus evaluated their antioxidant activity in a cellular context. To define the suitable concentration range, the cytotoxicity effects of **2–6** were determined by colorimetric MTT [3-(4,5-dimethyl-2-thiazolyl)-2,5-diphenyl-2H-tetrazolium bromide] assay [34] in human neuronal-like cells, SH-SY5Y. **1** was used as the reference compound. As reported in Fig. 2, treatment of SH-SY5Y cells with **4–6** (0.1–50 μM) did not show, as for **1**, modified cell viability. In contrast, 50 μM **3** and **2** produced a decrease of cell viability around

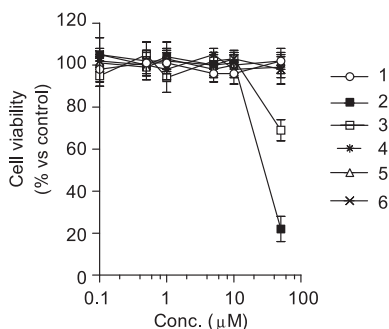


Fig. 2. Effects of compounds on cell viability in SH-SY5Y cells.

30% and 80%, respectively. In particular, the high cytotoxicity exerted by **2** deserves comment. It was previously reported that **7**, which is a fragment present in both **1** and **2**, was highly toxic in the same assay [18]. A comparison of these data with the toxicity profiles of compounds **1** and **2**, in which the abovementioned cytotoxic fragment was combined with LA and 5-(thiophen-2-yl)pentanoic acid, respectively, seems to support the hypothesis of a protective role for the LA dithiolane moiety.

The activity of **2–6** against intracellular ROS formation was then assessed in SH-SY5Y cells after treatment with *tert*-butyl hydroperoxide, a compound used to induce oxidative damage [35]. We used a range of concentrations of tested compounds that did not affect cell viability (1–50 μM for **4–6**; 1–10 μM for **2** and **3**). Treating SH-SY5Y cells with **4–6** showed a significant dose-dependent inhibitory effect on ROS formation (Table 2). Moreover, a relevant decrease of ROS production was observed for **3** with the highest concentration used (10 μM). In contrast, as expected, **2**, devoid of the LA moiety, did not reduce the intracellular ROS formation in SH-SY5Y cells.

Altogether, the cholinesterase and antioxidant activity data point to **4** as the lead compound of the present series of antioxidant MTDLs. In view of its structural similarity with prototypes **1** and memoquin, which are both effective inhibitors of AChE-induced Aβ aggregation, we checked if the anticholinesterase efficacy of **4** was accompanied by a concomitant inhibition of the proaggregating action of AChE. This was assessed through a thioflavin T-based fluorometric assay [36]. Data showed that **4** is a weak inhibitor of the AChE-induced Aβ aggregation (% inhibition at 100 μM = 16.8 ± 2.2), being significantly less potent than the

prototypes (% inhibition at 100 μM = 61.8 ± 0.8 and 87.1 ± 1.7 for **1** and memoquin, respectively). This finding is consistent with a lower anticholinesterase efficacy.

4. Conclusion

In the present investigation, we synthesized and studied a series of LA adducts, hypothesising that using diverse AChE motifs would offer a new point of diversity for MTDL development. The small difference between the inhibitory potencies of (*R*)- and (*S*)-**1** on AChE offered the rational basis for the synthesis of the new LA adducts as racemates. Of these, **4** emerged for its multiple biological properties, namely, inhibition of AChE activity in the sub-micromolar range and the ability to protect cells against oxidative stress. Interestingly, these properties were accompanied by the absence of a significant cytotoxicity in neuronal-like cells SH-SY5Y up to the highest concentration used (50 μM).

With respect to **1**, which represents a milestone in the field of MTDL development for Alzheimer's disease, **4** is characterized by a severe decrease in AChE inhibitory potency, followed by a significant reduction of AChE-induced anti-aggregating efficacy. This may suggest a reduction in multimodal efficacy of **4**, when compared to **1**; however, a more balanced activity profile has been attained here. In multitarget projects, it is critical to establish an optimal ratio of the desired activities, in order to maximize efficacy and safety. In particular, the profile of a lead compound should be balanced, so that each target is modulated *in vitro* to an equal or similar extent in the first instance [37]. However, the *in vivo* model proves to be much more complex, with many different factors contributing to the optimal level of activity for each target. Therefore, to verify whether or not **4** could be a new lead compound, *in vivo* feedback is needed.

5. Experimental

5.1. Chemistry

Melting points were taken in glass capillary tubes on Buchi SMP-20 apparatus and are uncorrected.

Direct infusion ESI-MS spectra were recorded on Perkin–Elmer 297 and Waters ZQ 4000 apparatus. ^1H NMR and ^{13}C -NMR spectra were recorded on Varian VXR 200, 300 and 400 instruments. Chemical shifts are reported in parts per millions (ppm) relative to tetramethylsilane (TMS), and spin multiplicities are given as s (singlet), br s (broad singlet), d (doublet), t (triplet), q (quartet) or m (multiplet). The elemental compositions of the compounds agreed to within $\pm 0.4\%$ of the calculated value. When the elemental analysis is not included, crude compounds were used in the next step without further purification. Chromatographic separations were performed on silica gel columns by flash (Kieselgel 40, 0.040–0.063 mm, Merck) or gravity (Kieselgel 60, 0.063–0.200 mm, Merck) column chromatography. Reactions were followed by thin-layer chromatography (TLC) on Merck (0.25 mm) glass-packed precoated silica gel plates (60 F254), then visualized in an iodine chamber or with a UV lamp. (*S*)-lipoic acid and (*R*)-lipoic acid were purchased from Waterstone Technology and Sigma Aldrich, respectively. The term “dried” refers to the use of anhydrous sodium sulfate. Compounds were named following IUPAC rules as applied by Beilstein-Institute AutoNom (version 2.1), a PC integrated software package for systematic names in organic chemistry.

5.1.1. General procedure for the synthesis of compounds **2–6**

A solution of the appropriate amine (1 eq, 0.1 M) and LA (1.5 eq) or 5-(thiophen-2-yl) pentanoic acid (1.5 eq) in dry DMF (5 mL), under N_2

was cooled to 0°C and then treated with 1-(3-dimethylaminopropyl)-3-ethylcarbodiimide hydrochloride (EDCI·HCl) (1.2 eq). The mixture was stirred at 0°C for further 15 min and then at rt for 2 h in the dark. Solvent was then removed under vacuum, avoiding heating up the reaction mixture while the lipoic fragment was present (**3–6**), affording an oily residue that was purified by gravity column.

5.1.1.1. Synthesis of *N*-(3-(6-chloro-1,2,3,4-tetrahydroacridin-9-ylamino)propyl)-5-(thiophen-2-yl)pentanamide (2**).** It was synthesized from *N*¹-(6-chloro-1,2,3,4-tetrahydroacridin-9-yl)propane-1,3-diamine [18] (**7**) (0.350 g, 1.21 mmol), and 5-(thiophen-2-yl)pentanoic acid (0.334 g, 1.82 mmol), and purified by flash chromatography. Elution with petroleum ether/ CH_2Cl_2 /MeOH/aqueous 30% ammonia (6.0:3.5:0.5:0.007) afforded **2** (0.441 g, 80%) as a yellowish wax. ^1H NMR (CDCl_3 , 200 MHz) δ 8.70 (br t, 1H, exchangeable with D_2O), 7.96 (d, J = 8.8 Hz, 1H), 7.88 (d, J = 2.2 Hz, 1H), 7.23 (d, J = 1.8 Hz, 1H), 7.09–7.11 (m, 1H), 6.91 (t, J = 3.6 Hz, 1H), 6.76–6.78 (m, 1H), 6.05 (br t, 1H, exchangeable with D_2O), 3.48–3.52 (m, 4H), 3.02–3.05 (m, 2H), 2.85 (t, J = 6.6 Hz, 2H), 2.71–2.76 (m, 2H), 2.25 (t, J = 6.6 Hz, 2H), 1.71–1.90 (m, 10H). ^{13}C NMR (CD_3OD , 100 MHz) δ 175.22, 156.59, 150.77, 144.54, 139.05, 138.60, 127.38, 126.26, 125.50, 123.88, 122.52, 117.81, 114.09, 112.26, 45.06, 35.72, 35.39, 31.12, 30.17, 29.01, 28.11, 25.04, 23.60, 21.54, 20.44. MS (ESI⁺) : m/z 456 [$\text{M}+1$]⁺. Anal. calcd for $\text{C}_{25}\text{H}_{30}\text{ClN}_3\text{OS}$: C, 65.84; H, 6.63; N, 9.21. Found: C, 65.61; H, 6.65, N, 9.18.

5.1.1.2. Synthesis of *N*-(3-(2-chloro-6,7-dimethoxyquinazolin-4-ylamino)propyl)-5-(1,2-dithiolan-3-yl)pentanamide (3**).** It was synthesised from **9** (0.15 g, 0.505 mmol) and LA (0.104 g, 0.505 mmol), and purified by gravity column chromatography. Elution with petroleum ether/ CH_2Cl_2 /EtOH/aqueous 30% ammonia (5:4.5:0.5:0.01) afforded **3** (0.110 g, 45%) as a yellowish oil. ^1H NMR (CDCl_3 , 300 MHz) δ 7.46 (br t, J = 5.8 Hz, 1H, exchangeable with D_2O), 7.34 (s, 1H), 7.14 (s, 1H), 6.22 (t, 1H, exchangeable with D_2O), 4.06 (s, 3H), 4.00 (s, 3H), 3.73 (q, J = 4.8 Hz, 2H), 3.58 (m, J = 6.3 Hz, 1H), 3.45 (q, J = 6.0 Hz, 2H), 3.24–2.91 (m, 2H), 2.53–2.42 (m, 1H), 2.32 (t, J = 7.5 Hz, 2H), 2.30–1.61 (m, 7H), 1.60–1.47 (m, 2H). ^{13}C -NMR (CDCl_3 , 75 MHz) δ 174.52, 160.58, 157.02, 155.07, 149.27, 147.93, 107.54, 107.22, 101.08, 56.63, 56.57, 56.47, 40.52, 38.74, 37.34, 36.78, 36.21, 34.86, 29.69, 29.13, 25.75. MS (ESI⁺) : m/z 486 [$\text{M}+1$]⁺. Anal. calcd for $\text{C}_{21}\text{H}_{29}\text{ClN}_4\text{O}_3\text{S}_2$: C, 52.00; H, 6.03; N, 11.55. Found: C, 52.23; H, 6.15, N, 11.67.

5.1.1.3. Synthesis of 5-(1,2-dithiolan-3-yl)-*N*-(6-(ethyl(2-methoxybenzyl)amino)hexyl)pentanamide (4**).** It was synthesized from *N*¹-ethyl-*N*¹-(2-methoxybenzyl)hexane-1,6-diamine [22] (**10**) (0.300 g, 1.13 mmol) and LA (0.350 g, 1.70 mmol), and purified by gravity column chromatography. Elution with a gradient of mobile phase petroleum ether/toluene/ CH_2Cl_2 /EtOH/aqueous 30% ammonia (7:2:1:1:0.05 to 7:1:1:1:0.05) afforded **4** (0.219 g, 43%) as a waxy solid. ^1H NMR (CDCl_3 , 200 MHz) δ 7.48–7.42 (m, 1H), 7.26–7.18 (m, 1H), 6.99–6.85 (m, 2H), 5.43 (br s, 1H, exchangeable with D_2O), 3.84 (s, 3H), 3.64–3.53 (m, 1H + s, 2H), 3.27–3.08 (m, 4H), 2.57–2.43 (m, 5H), 2.17 (t, J = 7.4 Hz, 2H), 2.00–1.82 (m, 1H), 1.73–1.29 (m, 14H), 1.07 (t, J = 7.0 Hz, 3H). ^{13}C -NMR (CDCl_3 , 100 MHz) δ 169.82, 157.78, 130.85, 128.76, 126.92, 120.56, 110.41, 56.70, 55.44, 55.34, 53.18, 51.15, 39.91, 39.16, 38.42, 36.42, 31.89, 29.65, 28.89, 28.85, 27.03, 26.66, 25.39, 14.09. MS (ESI⁺) : m/z 453 [$\text{M}+1$]⁺. Anal. calcd for $\text{C}_{24}\text{H}_{40}\text{N}_2\text{O}_2\text{S}_2$: C, 63.67; H, 8.91; N, 6.19. Found: C, 63.79; H, 8.93, N, 6.17.

5.1.1.4. Synthesis of the diastereomeric mixture of 5-(1,2-dithiolan-3-yl)-*N*-(3-((1-(3-methoxyphenyl)ethyl)(methyl)amino)propyl)pentanamide (5**).** It was synthesised from **13** (0.130 g, 0.59 mmol) and LA (0.240 g, 1.47 mmol), and purified by gravity column

chromatography. Elution with petroleum ether/CH₂Cl₂/EtOH/aqueous 30% ammonia (5.5:3.5:1:0.015) afforded **5** (0.133 g, 55%) as a waxy solid. ¹H NMR (CDCl₃, 200 MHz) δ 7.23 (t, *J* = 7.8 Hz, 1H), 6.90–6.75 (m, 3H), 6.56 (br s, 1H, exchangeable with D₂O), 3.79 (s, 3H), 3.58–3.47 (m, 2H), 3.25–3.05 (m, 4H), 2.45–2.37 (m, 3H), 2.20 (s, 3H), 2.03 (t, *J* = 7.2 Hz, 2H), 1.97–1.82 (m, 1H), 1.73–1.38 (m, 8H), 1.34 (d, *J* = 6.4 Hz, 3H). ¹³C-NMR (CDCl₃, 100 MHz) δ 172.42 (2C), 159.65 (2C), 129.32 (2C), 120.11 (2C), 113.76 (2C), 112.07 (4C), 64.08 (2C), 56.43 (2C), 55.21 (2C), 52.54 (2C), 40.22 (2C), 38.45 (2C), 37.98 (2C), 36.55 (2C), 34.64 (2C), 29.67 (2C), 28.93 (2C), 25.74 (2C), 25.47 (2C), 17.64, 17.60. MS (ESI⁺): *m/z* 411 [M+1]⁺. Anal. calcd for C₂₁H₃₄N₂O₂S₂: C, 61.42; H, 8.35; N, 6.82. Found: C, 61.65; H, 8.36, N, 6.81.

5.1.1.5. Synthesis of the diastereomeric mixture of *N*-(3-(3-(1-(dimethylamino)ethyl)phenoxy)propyl)-5-(1,2-dithiolan-3-yl)pentanamide (6**).** It was synthesized from **16** (0.150 g, 0.67 mmol) and LA (0.210 g, 1.02 mmol), and purified by gravity column chromatography. Elution with petroleum ether/toluene/CH₂Cl₂/MeOH/aqueous 30% ammonia (6:1:1.5:1.5:0.01) afforded **6** (0.080 g, 30%) as a waxy solid. ¹H NMR (CDCl₃, 200 MHz) δ 7.27 (t, *J* = 8.2 Hz, 1H), 6.98–6.78 (m, 3H), 5.99 (br t, 1H), 4.09 (t, *J* = 6.0 Hz, 2H), 3.62–3.21 (m, 5H), 3.19–3.05 (m, 3H), 2.53–2.40 (m, 1H), 2.32 (s, 6H), 2.22 (t, *J* = 7.2 Hz, 2H), 1.99–1.81 (m, 3H), 1.73–1.65 (m, 4H), 1.47 (d, *J* = 6.6 Hz, 3H). ¹³C-NMR (CDCl₃, 100 MHz) δ 172.88 (2C), 158.88, 158.77, 144.83, 144.25, 129.35 (2C), 120.26, 120.17, 113.56 (2C), 113.38 (2C), 66.24 (2C), 66.16 (2C), 65.91 (2C), 56.37 (2C), 43.04 (2C), 42.91 (2C), 40.18 (2C), 38.42, 37.23, 36.42 (2C), 34.58 (2C), 29.159 (2C), 28.95, 28.85, 25.61, 25.39, 19.99, 19.83. MS (ESI⁺): *m/z* 411 [M+1]⁺. Anal. calcd for C₂₁H₃₄N₂O₂S₂: C, 61.42; H, 8.35; N, 6.82. Found: C, 61.62; H, 8.36, N, 6.80.

5.1.2. Synthesis of *N*¹-(2-chloro-6,7-dimethoxyquinazolin-4-yl)propane-1,3-diamine (**9**)

A solution of the commercial 2,4-dichloro-6,7-dimethoxyquinazoline (1.00 g, 3.86 mmol) in anhydrous THF (15 mL) was added with propanediamine (0.572 g, 7.72 mmol). The resulting mixture was stirred at rt overnight. Evaporation of the solvent afforded a residue which was purified by gravity column. Elution with CH₂Cl₂/MeOH/aqueous 30% ammonia (9:1:0.2) afforded **9** (0.840 g, 75%) as a crystalline white solid. Mp = 210°–215 °C (dec.). ¹H NMR (CDCl₃, 200 MHz) δ 8.53 (br s, 1H, exchangeable with D₂O), 7.13 (s, 1H), 6.98 (s, 1H), 3.99 (s, 3H), 3.96 (s, 3H), 3.80 (q, *J* = 4.4 Hz, 2H), 3.10 (t, *J* = 5.6 Hz, 2H), 1.87 (m, 2H), 1.64 (br s, 2H, exchangeable with D₂O).

5.1.3. Synthesis of *tert*-butyl 3-((1-(3-methoxyphenyl)ethyl)(methylamino)propyl)carbamate (**12**)

A solution of 1-(3-methoxyphenyl)-*N*-methylethanamine [38] (**11**) (0.320 g, 1.9 mmol), *tert*-butyl 3-chloropropylcarbamate (0.370 g, 1.9 mmol), K₂CO₃ (0.260 g, 1.9 mmol) and a catalytic amount of KI in DMF (10 mL) was stirred under reflux conditions for 24 h. Evaporation of the solvent afforded a residue which was purified by gravity column. Elution with CHCl₃/MeOH/aqueous 30% ammonia (9:1:0.005) afforded **12** (0.245 g, 40%) as an oil. ¹H NMR (CDCl₃, 200 MHz) δ 7.20 (t, *J* = 8.0 Hz, 1H), 6.95–6.74 (m, 3H), 5.38 (br s, 1H, exchangeable with D₂O), 3.80 (s, 3H), 3.50 (q, *J* = 7.0 Hz, 1H), 3.13 (q, *J* = 6.2 Hz, 2H), 2.52–2.30 (m, 2H), 2.19 (s, 3H), 1.68–1.54 (m, 2H), 1.44 (s, 9H), 1.35 (d, *J* = 6.6 Hz, 3H).

5.1.4. Synthesis of *N*¹-(1-(3-methoxyphenyl)ethyl)-*N*¹-methylpropane-1,3-diamine (**13**)

A solution of **12** (0.230 g, 0.62 mmol) in CH₂Cl₂ (5 mL) was added with trifluoroacetic acid (1.5 mL). The reaction mixture was stirred at rt for 2 h and evaporated in vacuum. The obtained

residue was dissolved in water, made basic by adding 2 N NaOH and then extracted with CHCl₃ (3 × 20 mL) affording **13** as a white solid (0.137 g, quantitative yield). ¹H NMR (CDCl₃, 200 MHz) δ 7.27 (t, *J* = 8.0 Hz, 1H), 6.97–6.80 (m, 3H), 3.85 (s, 3H), 3.54 (q, *J* = 6.6 Hz, 1H), 2.74 (t, *J* = 6.6 Hz, 2H), 2.58–2.30 (m, 2H), 2.25 (s, 3H), 1.67–1.55 (m, 2H+2H exchangeable with D₂O), 1.39 (d, *J* = 7.0 Hz, 3H).

5.1.5. Synthesis of (*R,S*) 3-(1-(dimethylamino)ethyl)phenol (**14**)

Compound **14** was synthesised following the procedure described for the corresponding (*R,S*)-3-(1-(di-(²H₃)methylamino)ethyl)phenol in Ciszewska et al. [39]. A solution of methylamine hydrochloride in methanol was slowly added with KOH (3.48 g, 0.62 mol). After 20 min the hydroxyacetophenone (23.73 g, 0.174 mol) was added to the white precipitate formed and the mixture stirred at room temperature for 15 min. Over the next 30 min, a solution of NaCNBH₃ (4.13 g, 0.66 mol) in 50 ml of methanol was added dropwise to the imine intermediate, the mixture was stirred at rt for 30 min and further KOH (13.07 g, 0.233 mol) was added. After KOH was completely dissolved, the mixture was filtered and the filtrate concentrated under vacuum while keeping the temperature below 30 °C. Elution with a gradient of mobile phase EtOAc/aqueous 30% ammonia (10:0.07 to 10:0.2) afforded **14** (65%) as an oil. ¹H NMR (CDCl₃, 200 MHz) δ 9.08 (br s, 1H, exchangeable with D₂O), 7.15 (t, *J* = 7.6 Hz, 1H), 6.81–6.73 (m, 3H), 3.34 (q, *J* = 10.8 Hz, 1H), 2.25 (s, 6H), 1.42 (d, *J* = 6.4 Hz, 3H).

5.1.6. Synthesis of *tert*-butyl 3-(3-(1-(dimethylamino)ethyl)phenoxy)propylcarbamate (**15**)

A solution of **14** (0.350 g, 2.17 mmol), *tert*-butyl 3-chloropropylcarbamate (0.420 g, 2.17 mmol) and K₂CO₃ (0.300 g, 2.17 mmol) in DMF (10 mL) was stirred under reflux conditions for 24 h. Evaporation of the solvent afforded a residue which was purified by gravity column. Elution with CHCl₃/MeOH/aqueous 30% ammonia (9:1:0.02) afforded **15** (0.454 g, 65%) as an oil. ¹H NMR (CDCl₃, 200 MHz) δ 7.20 (t, *J* = 8.0 Hz, 1H), 6.79–6.89 (m, 3H), 4.92 (br s, 1H, exchangeable with D₂O), 4.02 (t, *J* = 6.4 Hz, 2H), 3.20–3.33 (m, 3H), 2.20 (s, 6H), 1.93–1.99 (m, 2H), 1.44 (s, 9H), 1.35 (d, *J* = 6.6 Hz, 3H).

5.1.7. Synthesis of 3-(3-(1-(dimethylamino)ethyl)phenoxy)propan-1-amine (**16**)

A solution of **15** (0.200 g, 0.62 mmol) in CH₂Cl₂ (5 mL) was added with trifluoroacetic acid (1.5 mL). The reaction mixture was stirred at rt for 2 h and evaporated in vacuum. The obtained residue was dissolved in water, made basic by adding 2 N NaOH and then extracted with CHCl₃ (3 × 20 mL). Evaporation of the dried solvent afforded **16** (0.137 g, quantitative yield). ¹H NMR (CDCl₃, 200 MHz) δ 7.20 (t, *J* = 8.0 Hz, 1H), 6.72–6.88 (m, 3H), 4.04 (t, *J* = 6.2 Hz, 2H), 3.12–3.22 (m, 1H), 2.91 (t, *J* = 6.6 Hz, 2H), 2.19 (s, 6H), 1.88–1.95 (m, 2H), 1.43 (br s, 2H, exchangeable with D₂O), 1.34 (d, *J* = 6.6 Hz, 3H).

5.1.8. Characterization of *S*-(5-([1,2]Dithiolan-3-yl)-*N* -[3-(6-chloro-1,2,3,4-tetrahydro-acridin-9-yl)amino]propyl)pentanamide) ((*S*)-**1**) and *R*-(5-([1,2]Dithiolan-3-yl)-*N* -[3-(6-chloro-1,2,3,4-tetrahydro-acridin-9-yl)amino]propyl)pentanamide) ((*R*)-**1**)

¹H NMR (CD₃OD, 400 MHz) δ 8.00 (d, *J* = 9.2 Hz, 1H), 7.62 (d, *J* = 2 Hz, 1H), 7.22 (dd, *J* = 9.2, 2.4 Hz, 1H), 3.48 (t, *J* = 7.2 Hz, 2H), 3.39–3.35 (m, 1H), 3.19 (t, *J* = 6.8 Hz, 2H), 3.05–2.91 (m, 2H), 2.85 (br m, 2H), 2.63 (br m, 2H), 2.32–2.24 (m, 1H), 2.07 (t, *J* = 7.6 Hz, 2H), 1.82–1.79 (m, 4H), 1.76–1.67 (m, 3H), 1.56–1.42 (m, 4H), 1.34–1.24 (m, 2H). ¹³C-NMR (CD₃OD, 100 MHz) δ 174.95, 158.36, 152.14, 146.46, 134.42, 125.14, 124.66, 123.88, 117.81, 115.48, 56.11, 45.20, 39.85, 37.90, 36.02, 35.47, 34.26, 32.47, 30.59, 28.45, 25.34, 24.60, 22.46, 21.99. MS (ESI⁺): *m/z* 478 [M+1]⁺.

(S)-1: Anal. calcd for $C_{24}H_{32}ClN_3OS_2$: C, 60.29; H, 6.75; N, 8.79; Found C, 60.53; H, 6.78; N, 8.65; (R)-1: Anal. calcd for $C_{24}H_{32}ClN_3OS_2$: C, 60.29; H, 6.75; N, 8.79; found C, 60.41; H, 6.73; N, 8.72.

Circular dichroism spectra of (S)-1 and (R)-1 were reported on Bertucci et al. [40].

5.2. Biology

5.2.1. Determination of the inhibitory potency on AChE and BuChE

The method of Ellman et al. [32] was followed. Compound 1, memoquin, rivastigmine and LA were used as reference compounds. Five different concentrations of each compound were used to obtain inhibition of AChE or BuChE activity comprising between 20% and 80%. The assay solution consisted of a 0.1 M phosphate buffer, pH 8.0, with the addition of 340 μ M 5,5'-dithio-bis(2-nitrobenzoic acid), 0.02 unit/mL human recombinant AChE or human serum BuChE (Sigma Chemical), and 550 μ M substrate (acetylthiocholine iodide or butyrylthiocholine iodide, respectively). Assay solutions with and without inhibitor were pre-incubated at 37 °C for 20 min followed by the addition of substrate. Blank solutions containing all components except AChE or BuChE were prepared in parallel to account for the non-enzymatic hydrolysis of the substrate. The reaction rates were compared, and the percentage of inhibition due to the presence of test compounds was calculated. Each concentration was analyzed in triplicate, and IC_{50} values were determined graphically from log concentration-inhibition curves.

5.2.2. Inhibition of AChE-induced A β 40 aggregation assay

A β 40 (2 mg mL⁻¹) was dissolved in HFIP and lyophilized. A 1 mM solution of tested inhibitor was prepared by dissolution in MeOH.

Aliquots of 2 μ L A β 40 peptide, lyophilized from 2 mg mL⁻¹ HFIP (1,1,1,3,3,3-hexafluoro-2-propanol) solution and dissolved in DMSO, were incubated for 24 h at room temperature in 0.215 M sodium phosphate buffer (pH 8.0) at a final concentration of 230 μ M. For co-incubation experiments aliquots (16 μ L) of hAChE (final concentration 2.30 μ M, A β /AChE molar ratio 100:1) and AChE in the presence of 2 μ L of the tested inhibitor (final inhibitor concentration 100 μ M) in 0.215 M sodium phosphate buffer pH 8.0 solution were added. Blanks containing A β 40 alone, recombinant hAChE alone, and A β 40 plus the tested inhibitor in 0.215 M sodium phosphate buffer (pH 8.0) were prepared. The final volume of each vial was 20 μ L. Each assay was run in duplicate. To quantify amyloid fibril formation, the thioflavin T fluorescence method was then applied [36]. The fluorescence intensities due to β -sheet conformation were monitored for 300 s at $\lambda_{em} = 490$ nm ($\lambda_{exc} = 446$ nm). The percent inhibition of the AChE-induced aggregation due to the presence of the tested compound was calculated by the following expression: $100 - (IF_i/IF_o \times 100)$ where IF_i and IF_o are the fluorescence intensities obtained for A β plus AChE in the presence and in the absence of inhibitor, respectively, minus the fluorescence intensities due to the respective blanks.

5.2.3. Cell cultures

Human neuronal like cells, SH-SY5Y, were routinely grown at 37 °C in a humidified incubator with 5% CO₂ in Dulbecco's modified Eagle's medium supplemented with 10% fetal calf serum, 2 mM glutamine, 50 U/ml penicillin and 50 μ g/mL streptomycin.

5.2.4. Determination of cytotoxicity

The cytotoxicity was evaluated with the colorimetric MTT [3-(4,5-dimethyl-2-thiazolyl)-2,5-diphenyl-2H-tetrazolium bromide] assay, as described by Mosmann et al. [34]. Briefly, SH-SY5Y cells were seeded in 96-well microtiter plates at 2×10^5 cells/well. After

24 h of incubation at 37 °C in 5% CO₂, the growth medium was removed and media containing compounds (0.1–50 μ M) were added to the cells. After 24 h of incubation, the cells were washed with phosphate buffered saline (PBS) and then incubated with MTT (5 mg/mL) in PBS for 4 h. After removal of MTT and further washing, the formazan crystals were dissolved with isopropanol. The amount of formazan was measured (405 nm) with a spectrophotometer (TECAN®, Spectra model Classic, Salizburg, Austria). The cell viability was expressed as percentage of control cells and calculated by the formula $F_t/F_{nt} \times 100$, where F_t = absorbance of treated neurones and F_{nt} = absorbance of untreated neurones.

5.2.5. Determination of antioxidant activity

The antioxidant activity of compounds was evaluated by measuring the formation of intracellular reactive oxygen species (ROS) evoked by exposure of SH-SY5Y cells to *tert*-butyl hydroperoxide (*t*-BuOOH), a compound used to induce oxidative stress. Formation of intracellular ROS was determined using a probe, 2',7'-dichlorodihydrofluorescein diacetate (DCFH-DA), as described by Wang H. et al. [35]. Briefly, SH-SY5Y cells were seeded in 96-well microtiter plates at 2×10^5 cells/well. After 24 h of incubation at 37 °C in 5% CO₂, the growth medium was removed and media containing compounds (1–50 μ M) were added to the cells. After 24 h of incubation, the cells were washed with PBS and then incubated with 5 μ M of DCFH-DA in PBS at 37 °C in 5% CO₂ for 30 min. After removal of DCFH-DA and further washing, the cells were incubated with 0.1 mM *t*-BuOOH in PBS for 30 min. At the end of incubation, the fluorescence of the cells from each well was measured ($\lambda_{exc} = 485$ nm, $\lambda_{em} = 535$ nm) with a spectrofluorometer (Wallac Victor® Multilabel Counter, Perkin Elmer Inc., Boston, MA). The results were expressed as percentage increase of intracellular ROS evoked by exposure to *t*-BuOOH and calculated by the formula $[(F_t - F_{nt})/F_{nt} \times 100]$, where F_t = fluorescence of treated neurones and F_{nt} = fluorescence of untreated neurones.

5.2.6. Statistical analysis

Data are reported as mean \pm SD of at least 3 independent experiments. Statistical analysis was performed using one-way ANOVA with Dunnett post hoc test. Differences were considered significant at $p < 0.05$. Analyses were performed using PRISM 3 software on a Windows platform.

Acknowledgments

This work was supported by grants from the University of Bologna (Italy). The authors thank Grace Fox for editing and proofreading the manuscript.

References

- [1] K.A. Jellinger, J. Neural Transm. Suppl. (2003) 101–144.
- [2] D. Pratico, Trends Pharmacol. Sci. 29 (2008) 609–615.
- [3] V. Calabrese, E. Guagliano, M. Sapienza, M. Panebianco, S. Calafato, E. Puleo, G. Pennisi, C. Mancuso, D.A. Butterfield, A.G. Stella, Neurochem. Res. 32 (2007) 757–773.
- [4] W.R. Markesbery, Free Radic. Biol. Med. 23 (1997) 134–147.
- [5] H.W. Querfurth, F.M. LaFerla, N. Engl. J. Med. 362 (2010) 329–344.
- [6] D. Pratico, S. Sung, J. Alzheimers Dis. 6 (2004) 171–175.
- [7] P.H. Reddy, M.F. Beal, Trends Mol. Med. 14 (2008) 45–53.
- [8] M.A. Smith, G. Perry, W.A. Pryor, Free Radic. Biol. Med. 32 (2002) 1049.
- [9] H.Y. Zhang, D.P. Yang, G.Y. Tang, Drug Discov. Today 11 (2006) 749–754.
- [10] A. Cavalli, M.L. Bolognesi, A. Minarini, M. Rosini, V. Tumiatti, M. Recanatini, C. Melchiorre, J. Med. Chem. 51 (2008) 347–372.
- [11] M.L. Bolognesi, M. Rosini, V. Andrisano, M. Bartolini, A. Minarini, V. Tumiatti, C. Melchiorre, Curr. Pharm. Des. 15 (2009) 601–613.
- [12] L. Holmquist, G. Stuchbury, K. Berbaum, S. Muscat, S. Young, K. Hager, J. Engel, G. Munch, Pharmacol. Ther. 113 (2007) 154–164.
- [13] J. Liu, Neurochem. Res. 33 (2008) 194–203.

- [14] A. Maczurek, K. Hager, M. Kenkies, M. Sharman, R. Martins, J. Engel, D.A. Carlson, G. Munch, *Adv. Drug Deliv. Rev.* 60 (2008) 1463–1470.
- [15] M.L. Bolognesi, A. Minarini, V. Tumiatti, C. Melchiorre, *Mini Rev. Med. Chem.* 6 (2006) 1269–1274.
- [16] M. Koufaki, A. Detsi, *Methods Mol. Biol.* 594 (2010) 297–309.
- [17] M. Decker, B. Kraus, J. Heilmann, *Bioorg. Med. Chem.* 16 (2008) 4252–4261.
- [18] M. Rosini, V. Andrisano, M. Bartolini, M.L. Bolognesi, P. Hrelia, A. Minarini, A. Tarozzi, C. Melchiorre, *J. Med. Chem.* 48 (2005) 360–363.
- [19] M. Rosini, V. Andrisano, M. Bartolini, Melchiorre, C. US7307083B2, 2007.
- [20] O. Tirosh, C.K. Sen, S. Roy, M.S. Kobayashi, L. Packer, *Free Radic. Biol. Med.* 26 (1999) 1418–1426.
- [21] A. Cavalli, M.L. Bolognesi, S. Capsoni, V. Andrisano, M. Bartolini, E. Margotti, A. Cattaneo, M. Recanatini, C. Melchiorre, *Angew. Chem. Int. Ed. Engl.* 46 (2007) 3689–3692.
- [22] M.L. Bolognesi, R. Banzi, M. Bartolini, A. Cavalli, A. Tarozzi, V. Andrisano, A. Minarini, M. Rosini, V. Tumiatti, C. Bergamini, R. Fato, G. Lenaz, P. Hrelia, A. Cattaneo, M. Recanatini, C. Melchiorre, *J. Med. Chem.* 50 (2007) 4882–4897.
- [23] M.L. Bolognesi, A. Cavalli, C. Bergamini, R. Fato, G. Lenaz, M. Rosini, M. Bartolini, V. Andrisano, C. Melchiorre, *J. Med. Chem.* 52 (2009) 7883–7886.
- [24] C. Melchiorre, V. Andrisano, M.L. Bolognesi, R. Budriesi, A. Cavalli, V. Cavrini, M. Rosini, V. Tumiatti, M. Recanatini, *J. Med. Chem.* 41 (1998) 4186–4189.
- [25] V. Tumiatti, V. Andrisano, R. Banzi, M. Bartolini, A. Minarini, M. Rosini, C. Melchiorre, *J. Med. Chem.* 47 (2004) 6490–6498.
- [26] V. Tumiatti, A. Milelli, A. Minarini, M. Rosini, M.L. Bolognesi, M. Micco, V. Andrisano, M. Bartolini, F. Mancini, M. Recanatini, A. Cavalli, C. Melchiorre, *J. Med. Chem.* 51 (2008) 7308–7312.
- [27] V. Tumiatti, M. Rosini, M. Bartolini, A. Cavalli, G. Marucci, V. Andrisano, P. Angeli, R. Banzi, A. Minarini, M. Recanatini, C. Melchiorre, *J. Med. Chem.* 46 (2003) 954–966.
- [28] M.L. Bolognesi, V. Andrisano, M. Bartolini, R. Banzi, C. Melchiorre, *J. Med. Chem.* 48 (2005) 24–27.
- [29] P. Bar-On, C.B. Millard, M. Harel, H. Dvir, A. Enz, J.L. Sussman, I. Silman, *Biochemistry* 41 (2002) 3555–3564.
- [30] A. Antonello, P. Hrelia, A. Leonardi, G. Marucci, M. Rosini, A. Tarozzi, V. Tumiatti, C. Melchiorre, *J. Med. Chem.* 48 (2005) 28–31.
- [31] A. Antonello, A. Tarozzi, F. Morroni, A. Cavalli, M. Rosini, P. Hrelia, M.L. Bolognesi, C. Melchiorre, *J. Med. Chem.* 49 (2006) 6642–6645.
- [32] G.L. Ellman, K.D. Courtney, V. Andres Jr., R.M. Feather-Stone, *Biochem. Pharmacol.* 7 (1961) 88–95.
- [33] N.H. Greig, T. Utsuki, D.K. Ingram, Y. Wang, G. Pepeu, C. Scali, Q.S. Yu, J. Mamczarz, H.W. Holloway, T. Giordano, D. Chen, K. Furukawa, K. Sambamurti, A. Brossi, D.K. Lahiri, *Proc. Natl. Acad. Sci. U S A* 102 (2005) 17213–17218.
- [34] T. Mosmann, *J. Immunol. Methods* 65 (1983) 55–63.
- [35] H. Wang, J.A. Joseph, *Free Radic. Biol. Med.* 27 (1999) 612–616.
- [36] M. Bartolini, C. Bertucci, V. Cavrini, V. Andrisano, *Biochem. Pharmacol.* 65 (2003) 407–416.
- [37] R. Morphy, C. Kay, Z. Rankovic, *Drug Discov. Today* 9 (2004) 641–651.
- [38] G.L. Grethe, L. His, M. Uskokovic, A. Brossi, *J. Org. Chem.* 33 (1968) 491–494.
- [39] G. Ciszewska, H. Pfefferkorn, Y.S. Tang, L. Jones, R. Tarapata, U.B. S., *J. Label. Compds. Radiopharm.* 39 (1997) 651–668.
- [40] C. Bertucci, A. De Simone, M. Pistolozzi, M. Rosini, *Chirality* (2011). doi:10.1002/Chir.21006.